Syrigou MS, Dow RS.

Strength of steel and aluminium alloy ship plating under combined shear and compression/tension.

***Engineering Structures* 2018, 166, 128-141.**

Strength of steel and aluminium alloy ship plating under combined shear and compression/tension

M.S. Syrigou*, R.S. Dow

Newcastle University, Newcastle Upon Tyne, UK

*Corresponding author. Address: School of Engineering, Armstrong Building, Newcastle University, Newcastle upon Tyne, NE1 7RU, U.K., Tel: +44 (0)191 208 8222

Email address: maria.syrigou@newcastle.ac.uk

Abstract

The load shortening curves are essential to the estimation of ultimate strength of ship structures under longitudinal bending in the simplified progressive collapse method. Longitudinal bending is the dominant load on ships structures, but in cases where the ship is heading to oblique seas and/or there are large openings in the structure due to its design (i.e. containerships) or due to damage (i.e. grounding, collision, blast), torsional loads may also be important when calculating ultimate strength and further investigation is required. Torsional loads on ship structures generate shear stresses which are carried primarily on the ship's plating, therefore the effect of shear on the in-plane load shortening behaviour of ship plating is thoroughly investigated in this paper. Initially, marine grade steel and aluminium alloy plates with different aspect ratio (1 to 4) and slenderness (1 to 5) are subjected only to shear loads. These results show that the plate aspect ratio does not significantly affect the progressive collapse behaviour of plates under shear, hence only square plates are investigated further. Steel and aluminium alloy square plates (5083-H116 and 6082-T6) with slenderness ratio 1 to 4 are subjected to shear, in-plane compression/tension and combined shear and compression/tension applying the same complex set of boundary conditions for all cases and using ABAQUS CAE. Finally, the generated interaction diagrams of shear and compressive/tensile loads provide essential information for the effect of shear on the progressive collapse of in-plane loaded plates allowing for the incorporation of torsion in the simplified progressive collapse method.

Keywords: plates, shear, compression, nonlinear finite element method, steel, aluminium

1. Introduction

A ship structure is mainly subjected to vertical hogging and sagging bending moment throughout its life due to extreme wave induced loading. However, when there are large openings in the structure due to wide hatch openings or due to damage, this inevitably results in reducing the torsional rigidity of the hull girder. The effect of torsional moment has been recognised to be important for ships with low torsional rigidity [1], especially in oblique seas. The torsional loads on the structure generate shear forces on the ship plating which does not affect the stiffeners of the panel.

Therefore, the shear effect on marine grade steel and aluminium alloy (5083-H116 and 6082-T6) ship plating with slenderness ratio (β) 1 to 5 is thoroughly investigated in this study. In Benson and Dow's study [2] the progressive collapse assessment of steel and aluminium plates and panels has been investigated taking into account the effect of initial imperfections, residual stresses and Heated Affected Zone (HAZ). Benson and Dow based on this data developed a code, ProColl (Progressive Collapse), for the progressive collapse assessment of ship structures under longitudinal bending. Therefore, the same parameters i.e. initial imperfections, residual stresses, material properties and HAZ for the plates are taking into account in this study aiming to future incorporation of torsional load into ProColl.

Initially, steel and aluminium plates (5082-H116) with slenderness ratio (β) 1 to 5 and aspect ratio (a/b) 1 to 4 are subjected only to shear load using the non-linear finite element method (NLFEM). The results show that the aspect ratio does not affect the progressive collapse behaviour of the plate under shear. Therefore, square plates which are assumed as the most conservative/severe estimate for the ultimate strength assessment of plates under in-plane compression are investigated further. A complex set of boundary conditions is applied for ship plating subjected only to axial compression/ tension and only to shear load. The ultimate strength of the plates under these loads is compared to experimental results, other studies and analytical formulas. Since,

these boundary conditions are validated, the plates are subjected to combined compressive/tensile and shear load.

Finally, the interaction diagrams of combined compression/tension and shear are generated for steel and aluminium alloys 5083-H116 and 6082-T6 ship plating with slenderness ratio (β) 1 to 6 investigating two cases for the unloaded edges, unrestrained and constrained edges. These diagrams do not only provide useful information for the progressive collapse behaviour of steel and aluminium alloy ship plating under combined compression/tension and shear but also are essential for the incorporation of torsion to the simplified progressive collapse method.

2. Background

In the literature, the ultimate strength of marine grade steel and aluminium alloy ship plating under in-plane compression/tension has been thoroughly investigated by different numerical approaches and experimental data. Plates subjected to shear loadings have been investigated mostly in the field of aeronautical and civil engineering and less by marine engineers. Finally, very few studies have been carried out to establish the criteria for plates under combined axial compressive/tensile and shear loads. The main studies and formulations which are taken into account for the establishment of the design criteria of steel and aluminium alloy ship plating under these loads are presented as follows:

2.1. Steel and aluminium alloy plates under axial compression/tension

Firstly, the Johnson-Ostenfeld formula, Eq. (1), provides correction due to plasticity for the elastic buckling stress formula, Eq. (2.1) to Eq. (2.2), calculating the critical/ultimate strength of steel and aluminium plates under axial compression.

$$\sigma_{cr} = \begin{Bmatrix} \sigma_E, & for\ \sigma_E \le 0.5\sigma_F \\ \sigma_F\,[1-\sigma_F/(4\sigma_E)], & for\ \sigma_E > 0.5\sigma_F \end{Bmatrix}, \begin{Bmatrix} \sigma_F = \sigma_o \\ \sigma_{E,\ Eq.\ (2.1)} \end{Bmatrix} \quad (1)$$

$$\sigma_E = \frac{k\pi^2}{12(1-\nu^2)}\left(\frac{t}{b}\right)^2 \quad (2.1)$$

$$k = [a/(m_o b) + m_o b/a]^2, \; where \; m_o = 1 \;\; for \; 1 \leq a/b \leq \sqrt{2} \qquad (2.2)$$

Secondly, Faulkner's formula, Eq. (3.1) to Eq. (3.2), a well-known and established empirical formula for predicting the collapse of simply supported unwelded steel plates with no constraints on the unloaded edges and average level of initial distortions ($0.12\beta^2 t$) [3]. Faulkner's formula can be also applied to aluminium plates under axial compression providing good correlation with other studies [2].

$$\begin{aligned} \frac{\sigma}{\sigma_o} &= \frac{2}{\beta} - \frac{1}{\beta^2}, \; \beta \geq 1 \\ \frac{\sigma}{\sigma_o} &= 1, \qquad \beta \leq 1 \end{aligned} \qquad (3.1)$$

$$\beta = \frac{b}{t}\sqrt{\sigma_o / E} \qquad (3.2)$$

where: σ = ultimate strength of the plate; σ_o= material yield stress; β = plate slenderness ratio defined by Eq. (3.2); b = plate width over which uniform compression is applied; t = plate thickness; E = Young's modulus; v = Poison's ratio

Furthermore, experimental and analytical/numerical studies by Frieze [4], Dow and Smith [5], [6], Chalmers [7] and Benson [2] have established the design criteria for steel plates in-plane loading. In these studies, the effect of boundary conditions, initial distortions and residual stresses on the ultimate strength has been investigated for a wide range of steel plates under compression with different aspect ratio (a/b) and slenderness ratio (β).

Finally, Eurocode 9 class 4 formulations, Eq. (4.1) to Eq. (4.9), and Paik & Duran's formula, Eq. (5), estimate the ultimate strength of marine aluminium alloy plates subjected to axial compressive loads. In addition, Little's [8], Mofflin and Dwight's [9] studies provide the background and design criteria for Eurocode 9 [10], while Hopperstad's [11], Kristensen's [12] and Benson's [2] studies provide a thorough investigation of aluminium alloy plates and comparison of their results with other studies.

The design value for compression force (N_{ED}) according to Eurocode 9 class 4 [10] should be equal to:

$$\frac{N_{ED}}{N_{Rd}} \leq 1.0 \qquad (4.1)$$

N_{RA}= design resistance to normal forces equal to:

$$N_{Rd} = \frac{A_{eff} \cdot \sigma_o}{\gamma_{M1}} \quad (4.2)$$

Assuming that N_{ED}= N_{Rd} and safety factor to account for design uncertainties (γ_{M1}) equal to 1, the design resistance N_{Rd} becomes:

$$N_{Rd} = A_{eff} \cdot \sigma_o \quad (4.3)$$

Where:

$$A_{eff} = 2b_{HAZ}\rho_{o_{HAZ}}t + (b - 2b_{HAZ})\rho_c t \quad (4.4)$$

$$\rho_{o_{HAZ}} = \frac{\sigma_{o_{HAZ}}}{\sigma_o} \quad (4.5)$$

$$\beta = \frac{C_1}{\left(\frac{\beta}{\varepsilon}\right)} - \frac{C_2}{\left(\frac{\beta}{\varepsilon}\right)^2} \quad (4.6)$$

$$C_1 = 29;\ C_2 = 198 \quad (4.7)$$

$$\beta = \frac{b}{t} \quad (4.8)$$

$$\varepsilon = \sqrt{250/\sigma_o} \quad (4.9)$$

The ultimate strength of aluminium plates subjected to compressive loads according to Paik and Duran's formulation [13] derives from Eq. (5) and β is defined in Eq. (3.2).

$$\frac{\sigma}{\sigma_o} = \begin{Bmatrix} -0.13\beta + 0.921, \beta < 3 \\ -0.07\beta + 0.741, \beta \geq 3 \end{Bmatrix} \quad (5)$$

2.2. Steel and aluminium alloy plates under shear

The critical shear stress of steel and aluminium plates under shear is estimated by Johnson-Ostenfeld formula, Eq. (6), which applies correction due to plasticity to the elastic shear stress formula for simply supported plates, Eq. (7).

$$\tau_{cr} = \begin{Bmatrix} \tau_E, & for\ \tau_E \le 0.5\sigma_F \\ \sigma_F\,[1-\sigma_F/(4\tau_E)], & for\ \tau_E > 0.5\sigma_F \end{Bmatrix}, \begin{Bmatrix} \sigma_F = \tau_Y = \sigma_Y/\sqrt{3} \\ \tau_{E,\ Eq.\ (7)} \end{Bmatrix} \quad (6)$$

$$\tau_E = \frac{k_s \pi^2 E}{12(1-v^2)} \left(\frac{t}{b}\right)^2,\ k_s = 5.3 + 4(a/b)^2\ \&\ a/b \ge 1 \quad (7)$$

Further studies on steel plates subjected to shear have been carried out by Rutherford and Zhang [14], Nara [15] and Paik [16] introducing formulations which derived from regression analysis and providing useful knowledge for the design criteria of plates under shear.

Zhang and Rutherford's equation for steel plates without taking into account residual stresses is described by Eq. (8) as follows:

$$\frac{\tau_u}{\tau_Y} = \begin{Bmatrix} 1, & for\ \beta_\tau < 1 \\ \frac{2}{\sqrt{\beta_\tau}} - \frac{1}{\beta_\tau}, & for\ \beta_\tau \ge 1 \end{Bmatrix}, \begin{Bmatrix} \beta_\tau = \frac{\beta}{1+(b/a)^{3/2}} \\ \tau_Y = \sigma_Y/\sqrt{3} \\ \beta_{,\ Eq.\ (3.2)} \end{Bmatrix} \quad (8)$$

Nara's equation, Eq. (9.1) to Eq. (9.2), derives from regression analysis of steel plates with average level of initial distortions and residual stresses under shear.

$$\frac{\tau_u}{\tau_Y} = \left(\frac{0.486}{\lambda}\right)^{1/3}, for\ 0.486 \le \lambda \le 2 \quad (9.1)$$

$$\lambda = \left(\tau_y/\tau_E\right)^{1/2} \quad (9.2)$$

Paik's empirical formula, Eq. (10), has taken into account steel plates with varying aspect ratio and thickness, average level of initial distortions and constrained edges which allow the sides of the plate to remain straight.

$$\frac{\tau_u}{\tau_Y} = \begin{cases} 1.324\left(\frac{\tau_E}{\tau_y}\right), & for\ 0 < \frac{\tau_E}{\tau_y} < 0.5 \\ 0.039\left(\frac{\tau_E}{\tau_y}\right)^3 - 0.274\left(\frac{\tau_E}{\tau_y}\right)^2 & \\ +0.676\left(\frac{\tau_E}{\tau_y}\right) + 0.388, & for\ 0.5 < \frac{\tau_E}{\tau_y} \leq 2 \\ 0.956, & for\ \frac{\tau_E}{\tau_y} > 2 \end{cases} \quad (10)$$

Where τ_E is the elastic critical shear stress which is given by Eq. (7).

Eurocode 3 [17] suggests also an empirical formulation for steel plates under shear, Eq. (11).

$$\frac{\tau_u}{\tau_Y} = \begin{cases} 1, & \lambda \leq 0.8 \\ 1 - 0.625(\lambda - 0.8), & 0.8 \leq \lambda \leq 1.2 \\ 0.9/\lambda, & \lambda \geq 1.2 \end{cases}, \{\lambda\ as\ defined\ by\ Eq.(9.2)\} \quad (11)$$

Finally, Eurocode 9 EN 1997 1-1 [10, p. 9] provides a series of formulations for the estimation of critical shear stress of aluminium plates, Eq. (12.1) to Eq. (12.6).

$$V_{ED} \leq V_{Rd} \quad (12.1)$$

If we assume that the design value of the shear force at the cross section (V_{ED}) is equal to the design shear resistance of the cross section (V_{Rd}) and the safety factor to account for design uncertainties (γ_{M1}) is equal to 1, then from Eq. (12.1) derives:

- For non-slender plates with $\beta \leq 39\varepsilon$, where β is defined by Eq. (4.8) and ε by Eq. (4.9), a yielding check is required using Eq. (12.2):

$$V_{Rd} = A_{net} \cdot \sigma_o / \left(\gamma_{M1}\sqrt{3}\right) \quad (12.2)$$

and net effective area (A_{net}) is equal to:

$$A_{net} = 2b_{HAZ}\frac{\sigma_{HAZ}}{\sigma_o}t + (b - 2b_{HAZ})\frac{\sigma_o}{\sigma_o}t \quad (12.3)$$

- For slender plates with > 39ε, where β is defined by Eq. (4.8) and ε by (4.9), yielding check is required using Eq. (12.2) and buckling check also using Eq. (12.4):

$$V_{Rd} = v_1 \cdot b \cdot t \cdot \sigma_o / \left(\gamma_{M1}\sqrt{3}\right) \quad (12.4)$$

Where:

$$v_1 = v_1 \cdot t \cdot \varepsilon \cdot \sqrt{k_t}/b < k_\tau \frac{430 \cdot t^2 \cdot \varepsilon^2}{b^2} \leq 1 \quad (12.5)$$

b = plate's breadth; a = plate's length;

$$k_\tau = 5.34 + 4.00 \cdot (b/a)^2, \ for \ a/b \geq 1 \quad (12.6)$$

2.3. Steel and aluminium alloy plates under combined axial compression/tension and shear

In the literature, the studies which examine plates subjected to compression/tension and shear are very limited. Both loads occur simultaneously, therefore a set of boundary conditions which allows these loads to be applied simultaneously is required. Harding [18] investigated steel plates under combined loads of shear and axial compression/tension using multi-layer/DR analysis. In this extensive research, the effect of the constraints at the unloaded edges, the level of initial imperfections and residual stresses as well plate's aspect ratio (a/b) and slenderness ratio (β) were taken into account for the strength assessment of steel plates.

Aluminium alloy plates under combined loads of axial compression/tension and shear were investigated by Dier [19] and Kristensen [12]. These studies have taken different parameters into account (i.e. initial geometric imperfections, residual stresses and HAZ) and present interaction diagrams of compressive and shear loads for aluminium plates.

3. Methodology

3.1. General approach

Previous work for steel and aluminium plates subjected to axial loads has shown that the collapse of square plates provides an excellent estimate of the strength of long plates subjected to axial loads. Therefore, in the

first part, the effect of aspect ratio on the progressive collapse behaviour of steel and aluminium plates under shear is investigated using NLFEM. Steel and aluminium plates with aspect ratio (a/b) 1 to 4 and slenderness ratio (β) 1 to 5 with constrained unloaded edges are subjected to shear and their results are shown similar progressive collapse behaviour with plates with different aspect ratio and same slenderness ratio. In the second part, only square steel and aluminium plates (1000x1000mm) are analysed examining both cases for their unloaded edges; unrestrained and constrained edges. A series of steel, aluminium alloy 5083-H116 and 6082-T6 plates with aspect ratio (a/b) equal to 1 and slenderness ratio (β) 1 to 6 is initially investigated under axial compression/tension and pure shear applying the same set of boundary conditions. These results are compared with analytical formulas and previous studies for plates under axial compression and under shear showing good correlation. Finally, this series of plates is subjected to axial compressive/tensile and shear loads simultaneously applying the same set of boundary conditions. In all cases, typical values of average initial imperfections and residual stresses for simply supported plates have been selected as producing conservative values of collapse load for plates under combined shear and axial load. In addition, the average level of magnitude for the initial distortions and residual stresses and the range of slenderness ratio values which has been chosen, represent typical values of welded plates in the ship industry (see paragraph 3.4).

3.2. Material properties

The stress-strain curves of steel, aluminium alloy 5083-H116 and aluminium alloy 5083-H116 in the heat affected zone (HAZ) are depicted in Fig.1. An elastic-perfectly plastic material behaviour was assumed for steel with yield stress $\sigma_o = 245MPa$, Young's Modulus $E = 207GPa$ and Poisson's number $v = 0.3$. The material behaviour of aluminium was described based on Ramberg-Osgood model approximation for the stress/strain curve, using Eq. (13) and 'knee factor' (*n*) equal to 15 and 30 for aluminium alloy 5083-H116 and 6082-T6 respectively. The 0.2% proof stress is $\sigma_{0.2} = 215MPa$ (5083-H116) and $\sigma_{0.2} = 260MPa$ (6082-T6), Young's Modulus $E = 70GPa$ and Poisson's number $v = 0.33$.

$$\varepsilon = \frac{\sigma}{E} + 0.002\left(\frac{\sigma}{\sigma_{0.2}}\right)^{n} \quad (13)$$

The stress-strain curve of both alloys in the Heat Affected Zone (HAZ) is described also by the same equation (Eq. (13)), but using a reduced proof yield stress ($\sigma_{0.2_{(HAZ)}}$) [2]. Therefore, the reduced proof yield stress was taken equal to:

5083-H116: $\sigma_{0.2_{(HAZ)}} = 0.67 \cdot \sigma_{0.2} = 0.67 \cdot 215 = 144.05MPa$

6082-T6: $\sigma_{0.2_{(HAZ)}} = 0.53 \cdot \sigma_{0.2} = 0.53 \cdot 260 = 130.91MPa$

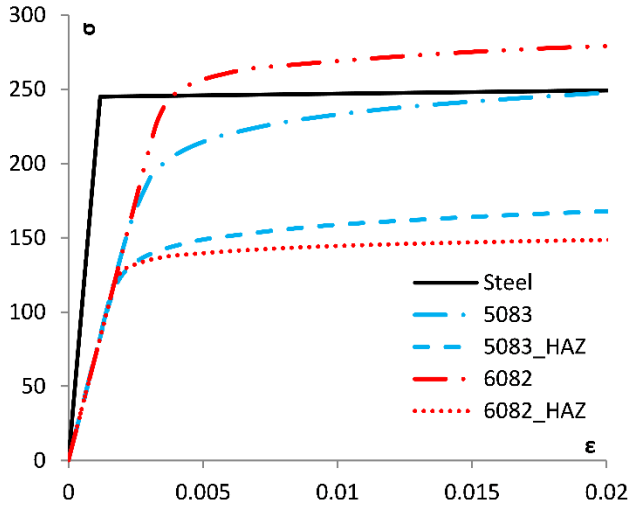

Fig.1. Stress-strain curves of steel, aluminium alloy 5083-H116, 6082-T6 and 5083-H116 & 6082-T6 in the HAZ

3.3. Mesh convergence study

All plates were modelled in ABAQUS using quadrilateral shell elements (S4R) with reduced integration which is valid for both thick and thin shell problems as previous studies have shown [20], [12], [2]. A mesh convergence study was conducted to select the element size. A square steel plate of slenderness ratio (β) equal to 3 and mesh size of 50mm, 20mm, 10mm and 5mm was examined under axial compression and pure shear. Its ultimate strength and critical shear stress are depicted in Fig. 2 and Fig.3 respectively and both of them show to converge for mesh size less than 20mm. Therefore, an element size of 10mm is suitable to balance for computational time and accuracy.

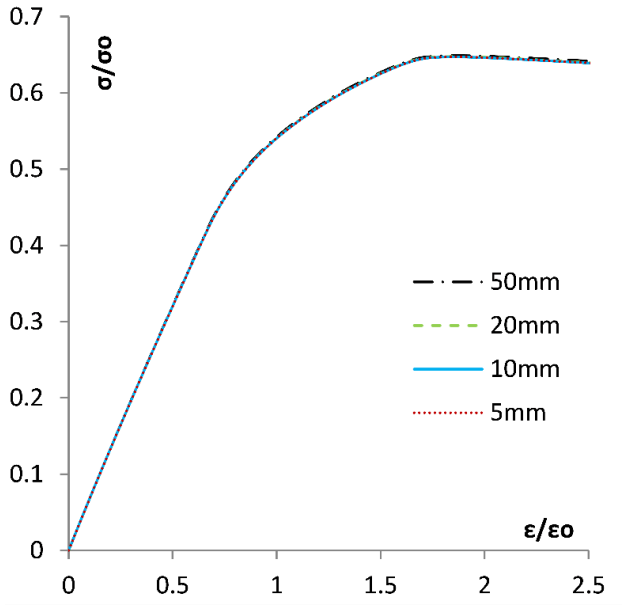

Fig. 2. Mesh convergence study for steel restrained plate (β=3) under axial compression

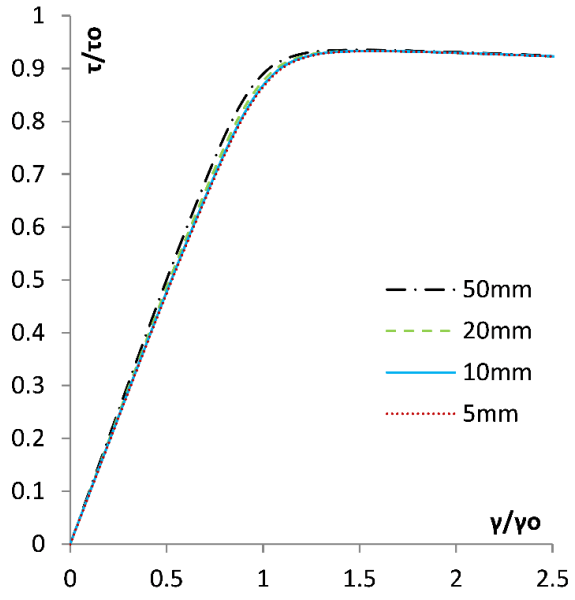

Figure 3. Mesh convergence study for steel restrained plates (β=3) under pure shear

3.4. Initial geometric imperfections

Previous studies [4], [6], [2] have proved the influence of initial geometric imperfections to the ultimate strength of ship plating. Hence, an average level of initial imperfections with maximum amplitude $w_o = 0.1\beta^2 t$ and Fourier series imperfection shape described by Eq. (14) were taken into account according to Dow's [5] and Benson's research ([2]. A typical representation combining 80% of a single half sine wave and 20% of a square half sine wave (m= square mode) has been used along plate's length and a single half sine wave along its width, in order to incorporate a realistic distortion of critical elastic buckling mode. However, in the case where aspect ratio of the plate is equal to 1, the shape of the imperfections is single half sine wave along in both directions as it is the most conservative case and it's described by Eq. (15). It is assumed that these initial distortion magnitudes and shapes represent typical values in ship's plating and will produce a reasonable assessment of the collapse behaviour of plates.

$$\frac{w}{w_o} = \left(0.8\sin\left(\frac{\pi x}{a}\right) + 0.2\sin\left(\frac{m\pi x}{a}\right)\right)\sin\left(\frac{\pi y}{b}\right),\ m = int\left(\frac{a}{b}\right) + 1 \qquad \text{Eq. (14)}$$

$$\frac{w}{w_o} = \sin\left(\frac{\pi x}{a}\right)\sin\left(\frac{\pi y}{b}\right),\ for\ a/b = 1 \qquad \text{Eq. (15)}$$

3.5. Residual stresses/Heat Affected Zone (HAZ)

The ultimate strength of steel plates under compression is affected by the tensile residual stress zone which is introduced to the plate due to welding [4], [6], [21], [2]. Therefore, this zone is modelled along the unloaded sides of the plate. The width of the tensile zone for steel was calculated in order to achieve equilibrium between the tensile area of stress equal to $0.95\sigma_o$ and the compressive area with average level of longitudinal residual stresses equal to $\sigma_{rc}/\sigma_o = -0.15$ [6].

The width of the Heat Affected Zone (HAZ) for aluminium plates was taken 25mm along the unloaded sides of the plate according to Benson's research [2], [12]. The tensile stress was assumed equal to $0.95 \cdot \sigma_{0.2_{(HAZ)}}$ and the compressive stresses were calculated as described in [2] in order to achieve equilibrium of the stresses on the plate. The effect of the HAZ on the proof stress of both aluminium alloys is also taken into account of as described in section 3.2 by a reducing proof stress.

3.6. Boundary conditions

A complex set of boundary conditions was developed in order to be valid not only for plates subjected to shear or axial compression/tension, but also in both loads simultaneously. These boundary conditions are developed to represent a simply supported case as would be expected to be experienced by ships plating in adjacent frame spaces of a ship's primary structure. The boundary conditions have been developed to fully represent the case of combined in-plane and shear loading with the unloaded edges either free to move in the in-plane direction or constrained to remain straight as would be the case where they are supported by a deep transverse girder and are fully described below. These boundary conditions would be expected to produce lower bound results for strength.

The application of uniform edge displacements to represent shear will imply that the shear strain is uniform along the edge, however during buckling this will produce a nonlinear distribution of shear load/ stress along the loaded edge.

In the first part, the aim is to apply shear load as displacement in x direction on edge 3 (Fig. 4). Therefore, all edges are simply supported. All nodes of edge 3 should have the same displacement in x direction, so they are constrained in x-direction. Additionally, edge 1 is fixed in x and z direction in order to fix the plate in the space and the unloaded edges (2 and 4) are constrained to remain straight but free to move in-plane. To clarify the boundary conditions of the unloaded edges, 'straight' means that all nodes e.g. at edge 2, retain the linearity of their displacement in x-direction between the corner nodes i.e. RP1 and RP4. The in-plane movement is free; however the nodes of the unloaded edges displace linearly in z direction between the corner nodes which depicts a realistic behaviour of the edges.

A relaxation step without load follows in order to obtain self-equilibrating residual stress distribution on the plate due to the initial distortions. In the first part, where only pure shear occurs, the load is applied as displacement in x direction on edge 3 using the Riks arc length.

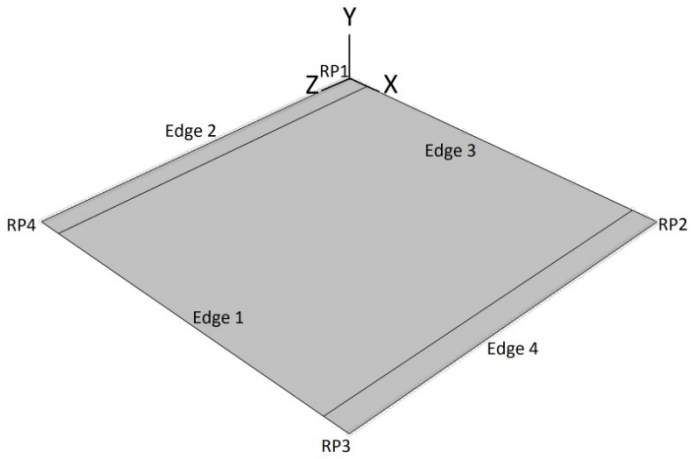

Fig. 4. Finite element model of plate

In the second part, where the shear and axial compression/tension are applied simultaneously, the boundary conditions were kept the same. However, the case of unrestrained unloaded edges was also investigated in which the edges 2 and 4 (Fig. 4) are not constrained to remain straight. A relaxation step was applied again before the load in order to self-equilibrate the stresses on the plate due to initial distortions. The load is applied as a uniform displacement on edge 3 in:

- Z direction for axial compression/tension;
- X direction for shear;
- Z and x direction simultaneously for combined loads of axial compression/ tension and shear;

4. Discussion / Results

4.1. Part 1: Ship plating with varying aspect ratio (a/b) 1 to 4 under pure shear.

The progressive collapse of steel and aluminium alloy 5083-H116 plates of slenderness ratio (β) 1 to 5 under pure shear is presented in Fig. 5 – Fig. 14. Plates with constrained unloaded edges and slenderness ratio (β) 1 to 5 are examined for a range of aspect ratio (a/b) 1 to 4. The average shear stress-shear strain curves of steel plates are presented in Fig. 5- Fig. 9 and aluminium alloy 5083-H116 plates in Fig. 10- Fig. 14, respectively.

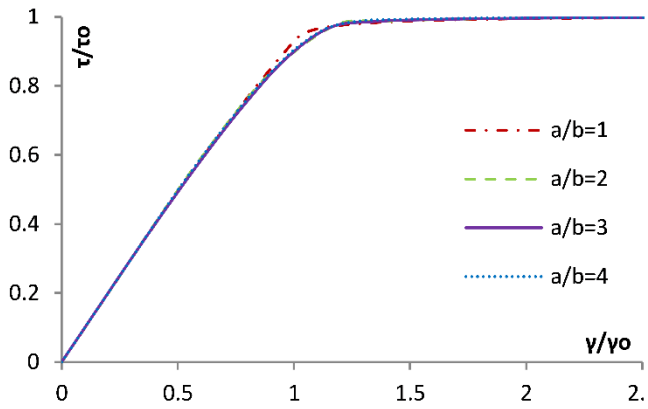

Fig. 5. Steel plates with β=1 and a/b=1-4 under pure shear.

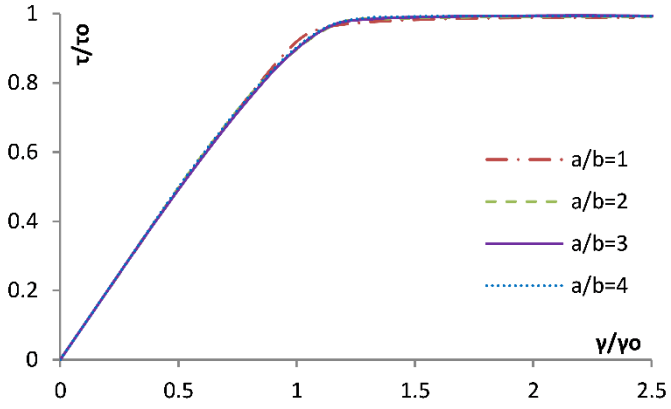

Fig. 6. Steel plates with β=2 and a/b=1-4 under pure shear.

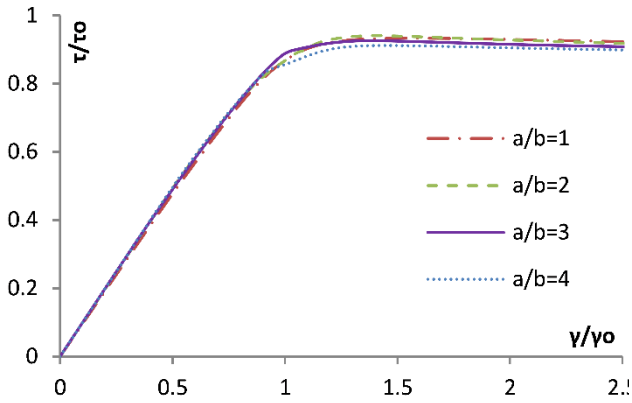

Fig. 7. Steel plates with β=3 and a/b=1-4 under pure shear.

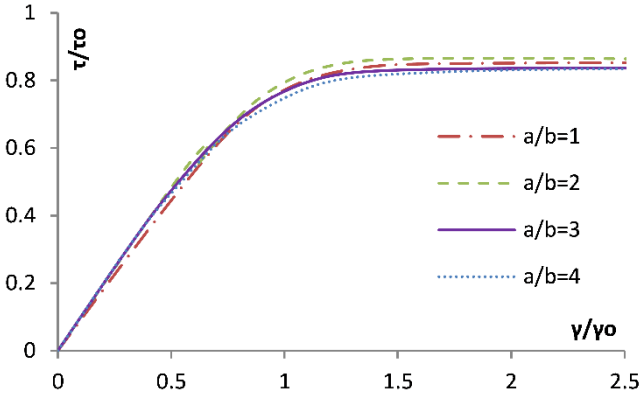

Fig. 8. Steel plates with β=4 and a/b=1-4 under pure shear.

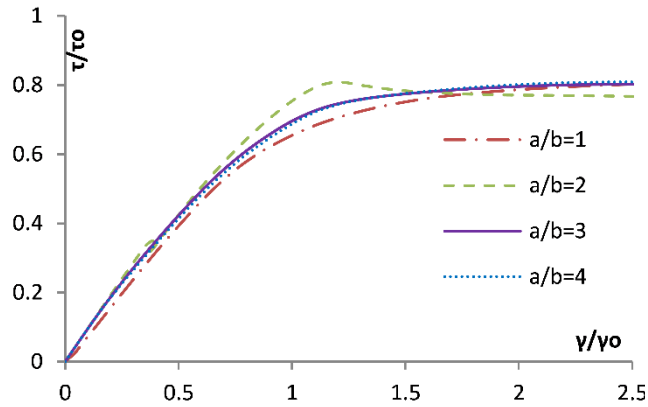

Fig. 9. Steel plates with β=5 and a/b=1-4 under pure shear.

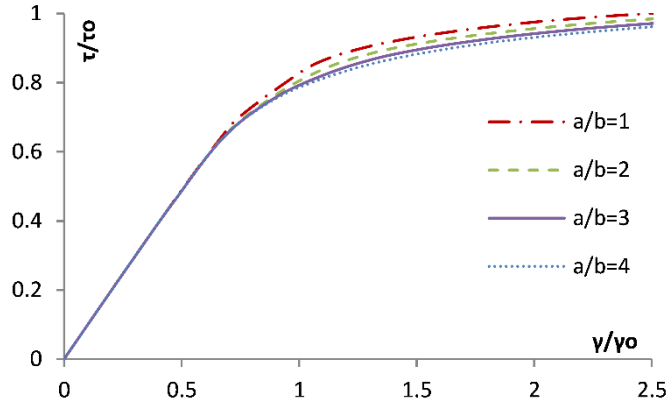

Fig. 10. Aluminium alloy 5083-H116 plates with β=1 and a/b=1-4 under pure shear.

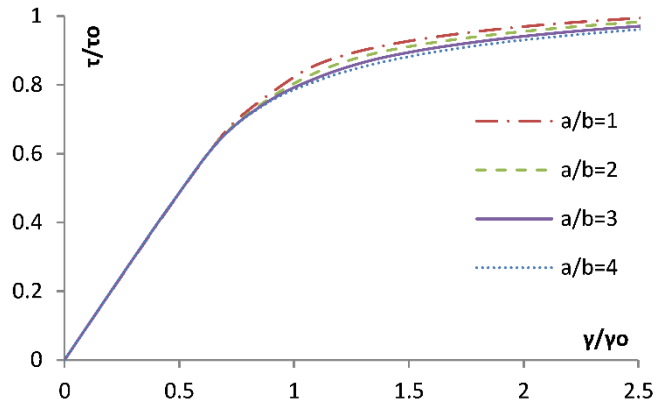

Fig. 11. Aluminium alloy 5083-H116 plates with β=2 and a/b=1-4 under pure shear.

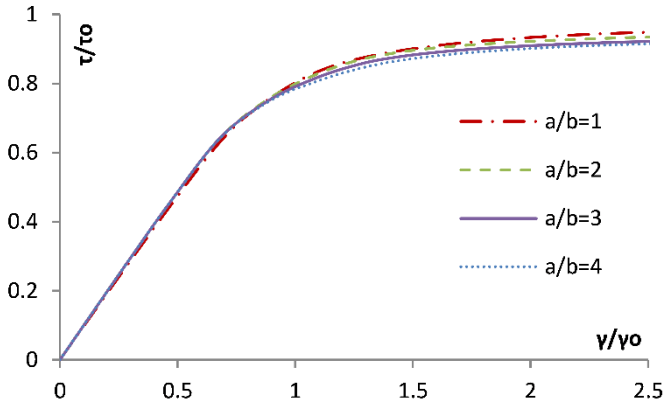

Fig.12. Aluminium alloy 5083-H116 plates with β=3 and a/b=1-4 under pure shear.

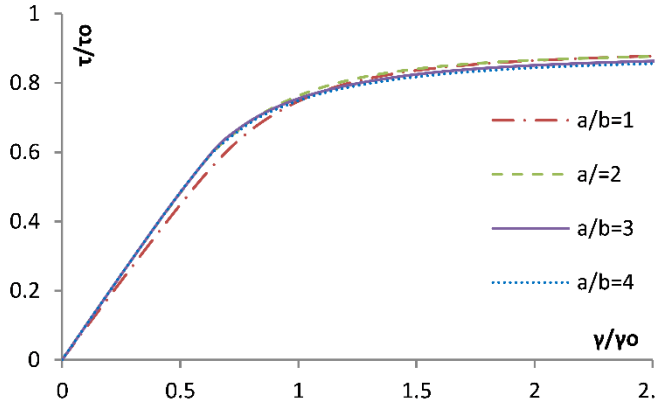

Fig. 13. Aluminium alloy 5083-H116 plates with β=4 and a/b=1-4 under pure shear.

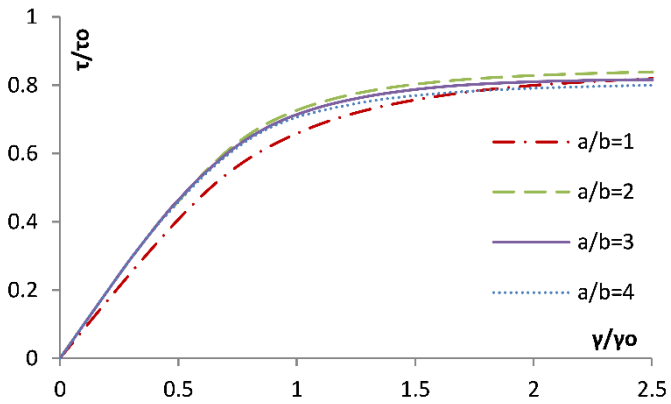

Fig. 14. Aluminium alloy 5083-H116 plates with β=5 and a/b=1-4 under pure shear.

The progressive collapse behaviour of constrained plates under shear seems to be independent of the aspect ratio (a/b) of plates with slenderness ratio (β) 1 to 4 for both steel and aluminium alloys, Fig. 5- Fig. 9 and Fig. 10 – Fig. 14, respectively. Fig. 9 & Fig. 14 show that only very slender plates, with slenderness ratio (β) equal to 5, demonstrate a small effect due to aspect ratio. However, these plates (β=5) are very slender and they are not particularly used as ship plating [7].

4.2. Part 2: Square ship plating under combined loads of axial compression/tension and shear.

In this part, the progressive collapse behaviour of square (1000x1000mm) steel and aluminium alloy plates (5083-H116 and 6082-T6) under axial compression/tension, pure shear and combined loads of axial compression/tension and shear is investigated using finite element analysis. Initially, the plates are subjected

only to axial compression/tension and to pure shear in order to investigate the effect of the constrained and unrestrained unloaded edges on the progressive collapse of the plate. The stress-strain curves of both cases are presented and the results are compared to well-known analytical methods and studies which are mentioned in the background.

Finally, the plates are subjected to axial compressive/tensile and shear load simultaneously and the interaction diagrams of these combined loads are generated for steel, aluminium alloy 5083-H116 and 6082-T6 plates with slenderness ratio (β) 1 to 6.

4.2.1.Steel, aluminium alloy 5083-H116 and 6082-T6 plates under axial compression/tension

A series of steel, aluminium alloy 5083-H116 and 6082-T6 plates with slenderness ratio (β) 1 to 6 is subjected to in-plane compression and tension. As it has already mentioned, two cases are examined for unloaded edges; one in which are free to move in plane (unrestrained) and another one in which are constrained to remain straight (constrained). The stress-strain curves of these plates under pure compression/tension are presented in Fig. 15 – Fig. 20 for a range of slenderness ratio (β) 1 to 6.

The load shortening curves of steel square plates are depicted in Fig. 15 & Fig. 16 for unrestrained and constrained edges, respectively. It seems that constrained plates become stiffer than unrestrained due to the constraints of unloaded edges, with a resulting increase in ultimate strength. However, this is not the case for very stocky plates (β=1) which fail though plastic yielding and their ultimate strength is independent from the boundary conditions on the unloaded edges.

Similar pattern to steel plates under direct in-plane compression and tension seems to follow aluminium alloy 5083-H116 and 6082-T6 plates (Fig. 17 to Fig. 20). Non-stocky constrained aluminium plates present higher values of compressive and tensile stress which may sustain and become stiffer in comparison to unrestrained plates. In addition, there are no particular differences in the behaviour between alloy 5083-H116 and 6082-T6 plates with the same boundary conditions, unrestrained (Fig.17 & Fig. 19) and constrained (Fig. 18 & Fig. 20) under compression/ tension.

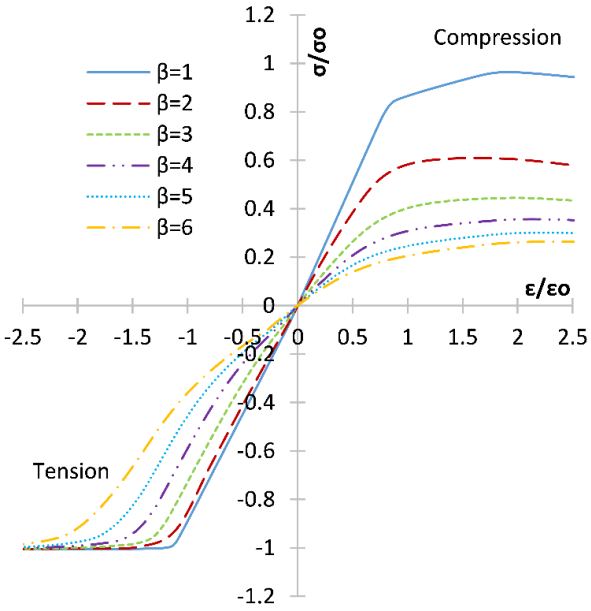

Fig. 15. Stress-strain curves of unrestrained steel plates under axial compression/tension.

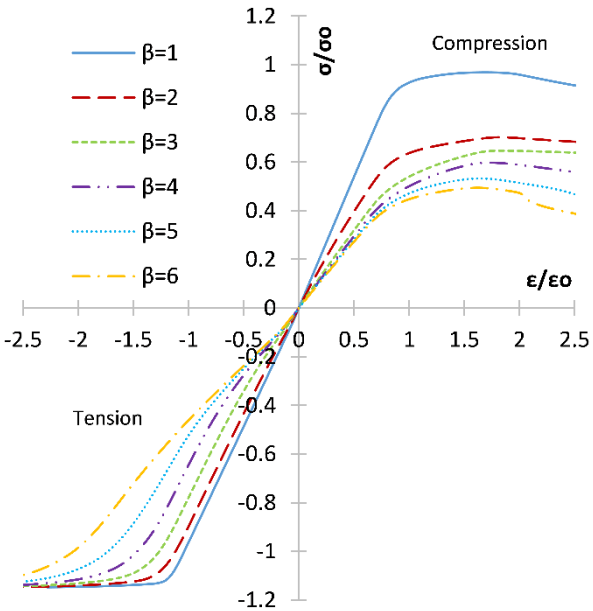

Fig. 16. Stress-strain curves of constrained steel plates under axial compression/tension.

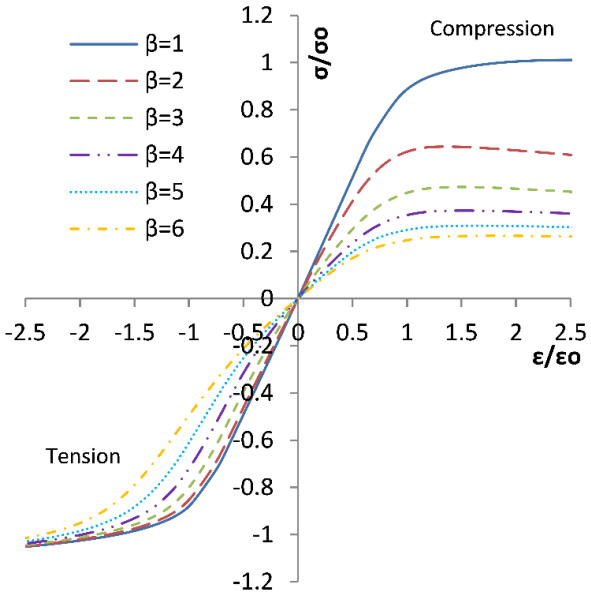

Fig. 17. Stress-strain curves of unrestrained aluminium alloy 5083-H116 plates under axial compression/tension.

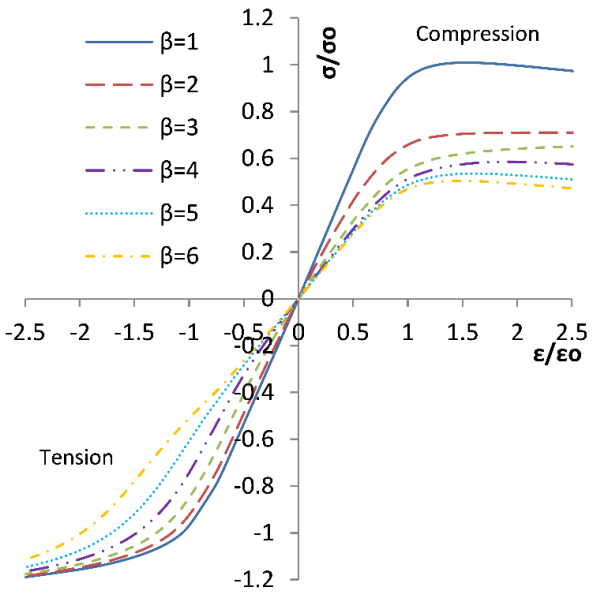

Fig. 18. Stress-strain curves of constrained aluminium alloy 5083-H116 plates under axial compression/tension.

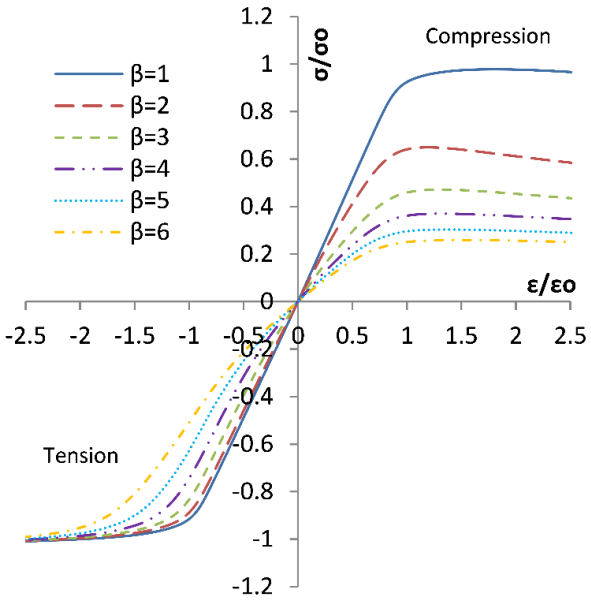

Fig. 19. Stress-strain curves of unrestrained aluminium alloy 6082-T6 plates under axial compression/tension

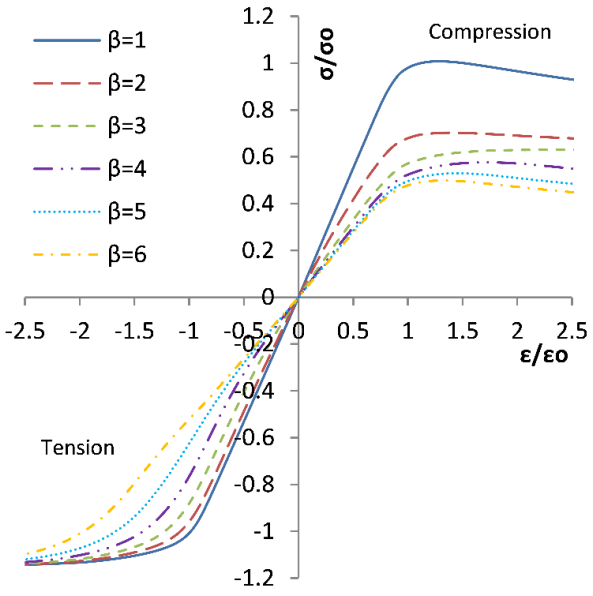

Fig. 20. Stress-strain curves of constrained aluminium alloy 6082-T6 plates under axial compression/tension

4.2.2.Steel, aluminium alloy 5083-H116 and 6082-T6 plates under pure shear.

The same series of steel and aluminium plates which was investigated under compression/shear in section 4.2.1 was also subjected to pure shear. The critical shear stress-shear strain curves of this series are presented in Fig. 21 to Fig. 26. The behaviour of stocky (β=1, 2) steel unrestrained plates remains unaffected by the boundary conditions of unloaded edges and failure occurs due to shear yielding (Fig. 21). Critical shear stress decreases as plate becomes more slender and shear buckling occurs. The shear stress-strain curves of constrained steel plates (Fig. 22) follow similar pattern but slender plates (β>2) show increased critical shear stress and stiffness in comparison with unrestrained plates.

The behaviour of aluminium alloy 5083-H116 (Fig. 23 & Fig. 24) and 6082-T6 (Fig. 25 & Fig. 26) plates does not differ from this of steel plates under pure shear. The shear stress- strain curves show shear stress to increase as plate becomes more slender, stocky plates not to be affected by the boundary conditions of unloaded edges and only slender plates are affected becoming stiffer and increasing their critical shear stress.

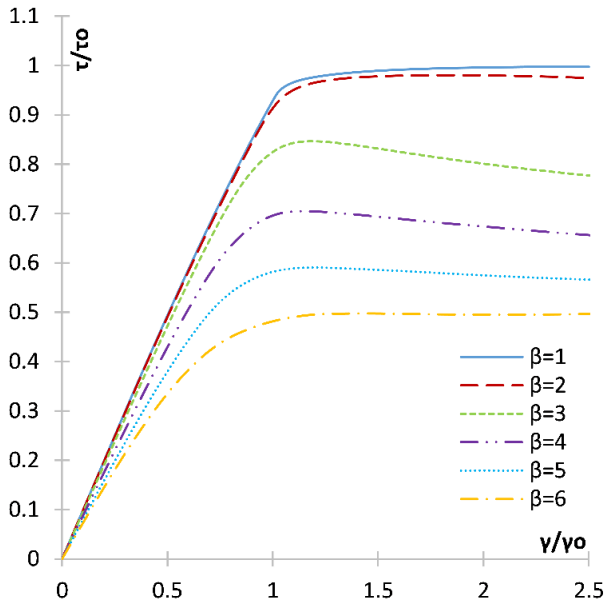

Fig. 21. Shear stress-shear strain curves of unrestrained steel plates under pure shear.

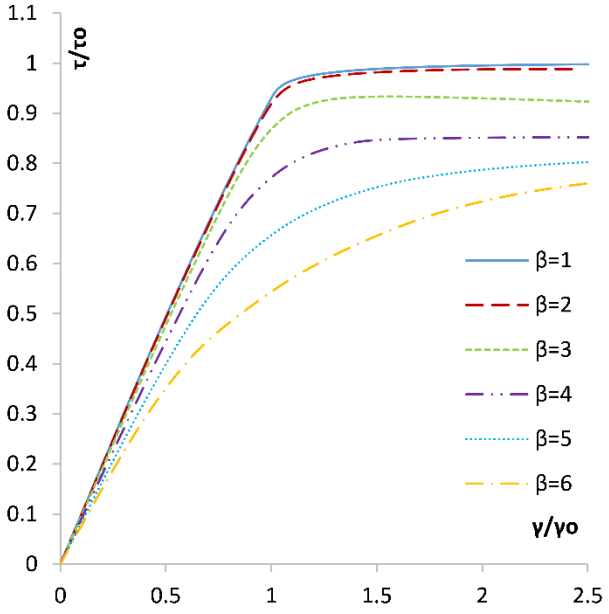

Fig. 22. Shear stress-shear strain curves of constrained steel plates under pure shear.

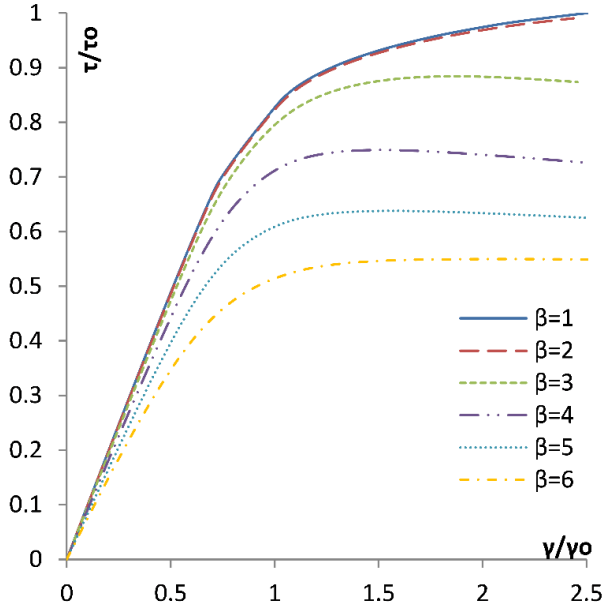

Fig. 23. Shear stress-shear strain curves of unrestrained aluminium alloy 5083-H116 plates under pure shear.

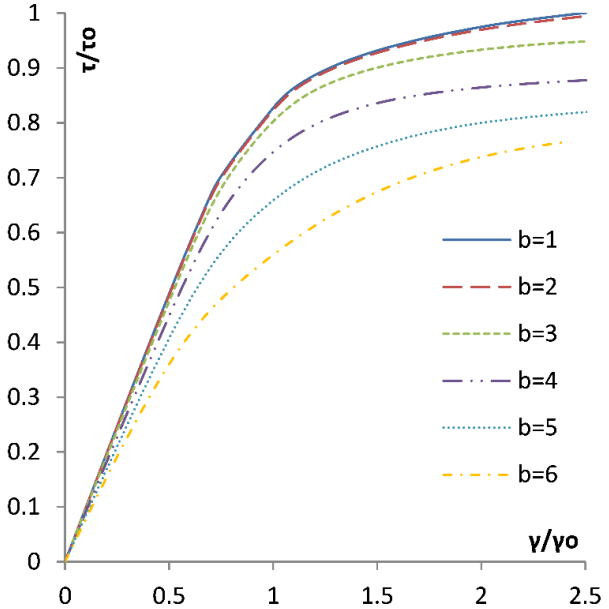

Fig. 24. Shear stress-shear strain curves of constrained aluminium alloy 5083-H116 plates under pure shear.

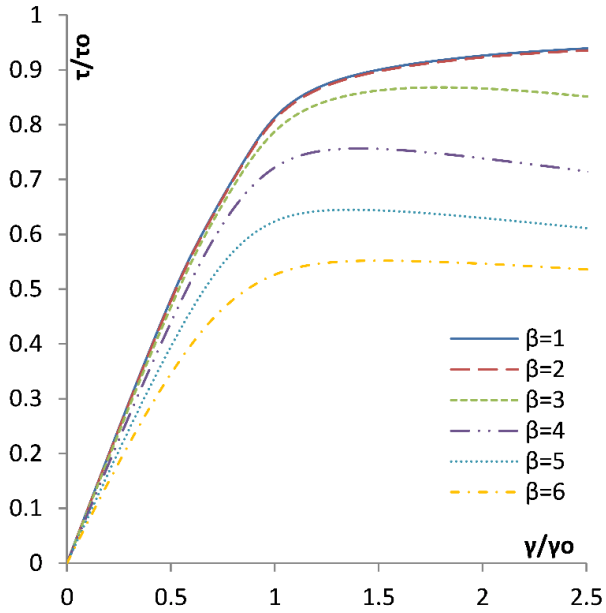

Fig. 25. Shear stress-shear strain curves of unrestrained aluminium alloy 6082-T6 plates under pure shear.

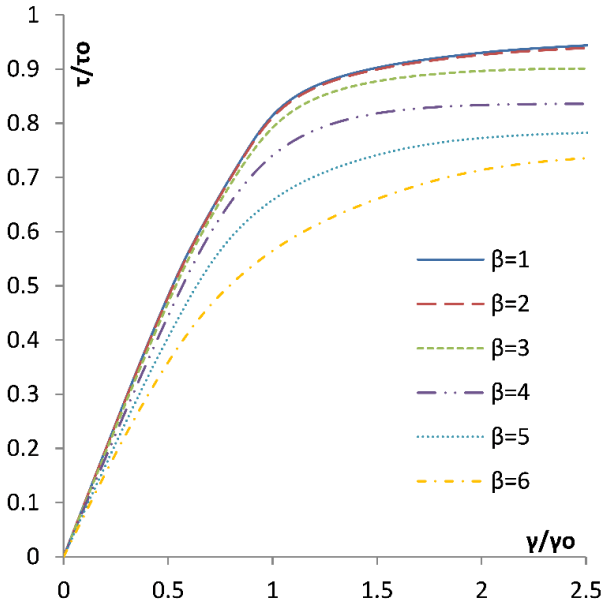

Fig. 26. Shear stress-shear strain curves of constrained aluminium alloy 6082-T6 plates under pure shear.

4.2.3.Comparison of ultimate strength and critical shear stress of steel, aluminium alloy 5083-H116 and 6082-T6 plates with theoretical formulas and previous studies

A comparison of the nonlinear finite element results of ultimate strength of plates under pure axial compression and pure shear with relevant theoretical formulas and other studies was taken part. The purpose of this comparison is to validate the boundary conditions which are applied to plate models under combined loads of compression/ tension and shear, since are the same with these of separate load cases of axial compression and pure shear.

The direct stress of unrestrained steel plates under axial compression is compared with Chalmers' results, Faulkner's theoretical formula (Eq. (3.1)) and critical elastic stress formulation with corrected plasticity by Johnson-Ostenfeld (Eq. (1)) in Fig. 27. All of these formulas and studies are referring or have been applied to unrestrained plates. The graph of the F.E. results for unrestrained plates shows a good correlation with Faulkner's theoretical values and Chalmers's results as it follows the same pattern and does not overestimate plates' ultimate strength. Differences are expected as we compare F.E. results with theoretical values (Faulkner) and a different study (Chalmers') in which all parameters and analysis are not exactly the same.

The critical elastic stress formulation with corrected plasticity by Johnson-Ostenfeld estimates critical elastic direct stress which is much lower than plate's ultimate strength when buckling occurs in the elasto-plastic area for slender plates (β>2). However, in the case of stocky plates (β<2) which yield in plasticity region, Johnson-Ostenfeld formulation agrees well with the rest studies and formulas.

The nonlinear finite element results of plates with constrained edges are also presented in Fig. 27. Stocky plates (b<2) which their ultimate strength is not affected by constraints on the unloaded edges show good correlation with the compared formulas and studies which are referring to unrestrained plates. The collapse stress of slender plates (β>2) is higher due to the constrained edges which provide additional strength to the plate. In addition, these findings agree with Frieze's study on the ultimate load behaviour of plates in compression [4].

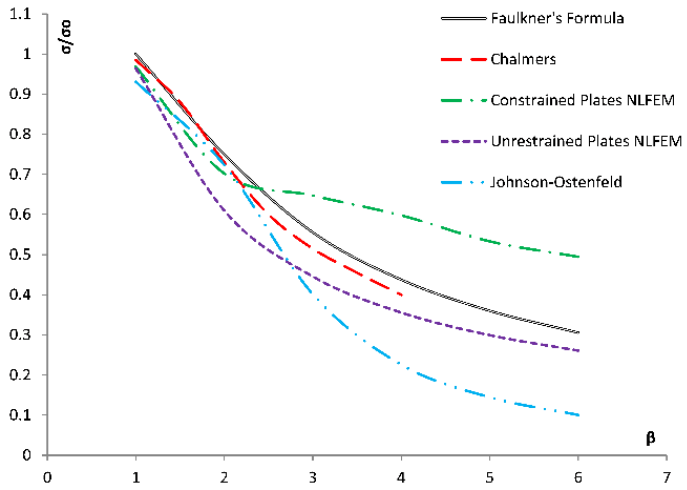

Fig. 27. Comparison of NLFEM results of the current study with other studies and theoretical values of ultimate strength of steel plates under axial compression.

The critical shear stress of both unrestrained and constrained steel plates under pure shear is compared with theoretical formulas proposed by Nara (Eq. (9.1)), Johnson-Ostenfeld (Eq. (6)), Paik and Thayamballi (Eq. (10)), Zhang (Eq. (8)) and Eurocode 3 (Eq. (11)) in Fig. 28. All formulations are referred to constrained plates and provide the critical shear stress except Johnson-Ostenfeld's formulation. This formulation estimates the elastic shear stress of plates with correction due to plasticity which is lower than ultimate shear stress. The ultimate

shear stress of stocky plates (β<2) according to all formulations and F.E. results does not particularly differ. Unrestrained slender plates (β>2) are affected by the boundary conditions of unloaded edges and its critical shear stress is decreasing much more than this of constrained plates. The graph of slender constrained plates follows similar pattern to Zhang's, Nara's, Paik and Thayamballi's and Eurocode 3 formulations. The critical shear stress for plates with slenderness ratio (β) equal to 3 show very good agreement with the developed empirical formula by Paik and Thayamballi (Eq. (10)) and for plates with slenderness ratio (β) more than 4 with Nara's formulation (Eq. (9.1)).

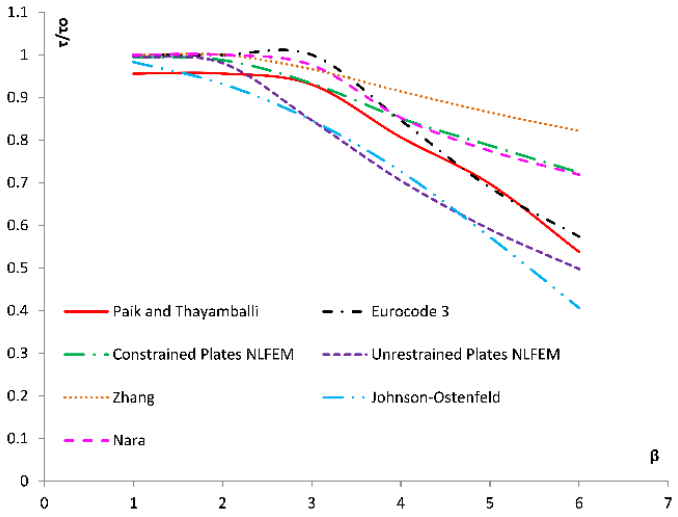

Fig. 28. Comparison of NLFEM results of the current study with other studies and theoretical values of the critical shear stress of steel plates under pure shear.

Aluminium alloys 5083-H116 and 6082-T6 plates under axial compression are compared with theoretical formulations in Fig. 29 and Fig. 30, respectively. Both aluminium alloys 5083-H116 and 6082-T6 present similar behaviour under axial compression, therefore only the behaviour of 5083-H116 is analysed in detail and any difference which occurs with 6082-T6 is commented.

The ultimate strength of unrestrained and constrained aluminium alloy plates is compared with Faulkner's formula (Eq. (3.1)), Eurocode 9 (Eq. (4.1) – Eq. (4.9)) and Paik and Duran's formulation (Eq. (5)) in Fig. 29 and Fig. 30. The graph of unrestrained plates presents similar pattern to Faulkner's empirical formula for unrestrained plates and Eurocode 9 results. The ultimate strength of stocky constrained plates (β<2) is not

affected by the boundary conditions of the unloaded edges and it decreases as the plate becomes more slender but much less than in the case of unrestrained edges. Paik and Duran's graph for slender plates (β>2) is close to Faulkner's, Eurocode 9 and the F.E. graph for unrestrained plates but following different slope.

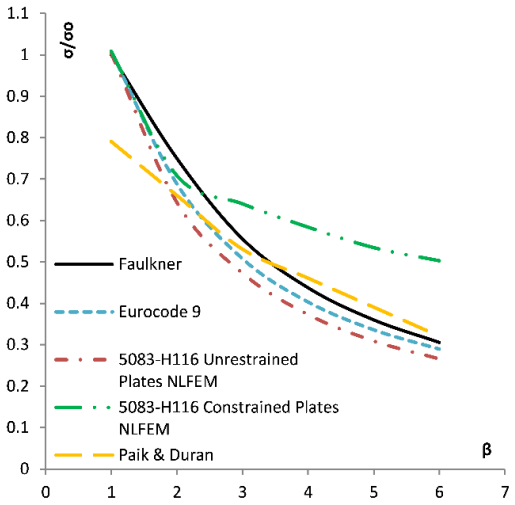

Fig. 29. Comparison of NFEM results of the current study with theoretical values of the ultimate strength of aluminium alloy 5083-H116 plates under axial compression.

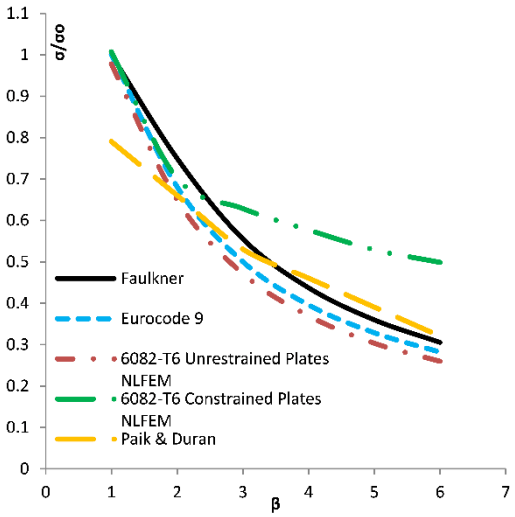

Fig. 30. Comparison of F.E. results of the current study with other theoretical values of the ultimate strength of aluminium alloy 6082-T6 plates under axial compression.

The critical shear stress of aluminium alloys 5083-H116 and 6082-T6 plates under pure shear is compared with Eurocode 9 formulas (Eq. (12.1)- eq. (12.6)) in Fig.31 and Fig. 32, respectively. Stocky plates (β<2) subjected to shear are also independent from the boundary conditions at the edges. Constrained slender plates withstand higher levels of critical shear stress than unrestrained plates. However, the graphs in both cases have similar curvature.

Eurocode's 9 formulations for non-slender plates estimate critical shear stress due to yield and an additional buckling check is required for slender plates. The estimated critical shear stress for non-slender plates (β<2) according to Eurocode's 9 formulations is higher than the non-linear finite element results but both graphs follow the same pattern, a straight horizontal line. The buckling shear stress of slender plates (β>2) shows similar tendency with the non-linear finite element results.

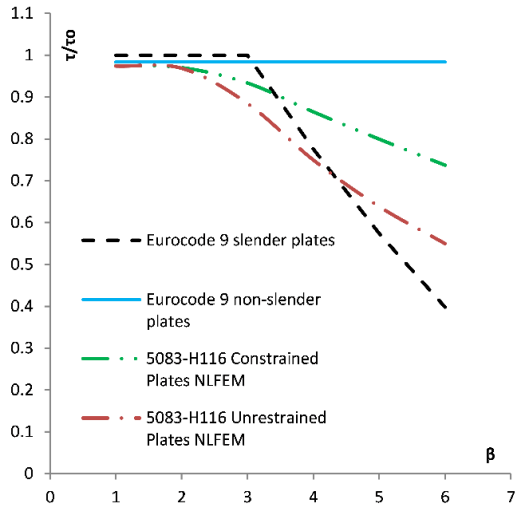

Fig. 31. Comparison of NFEM results of the current with theoretical values of the critical shear stress of aluminium alloy 5083-H116 plates under pure shear.

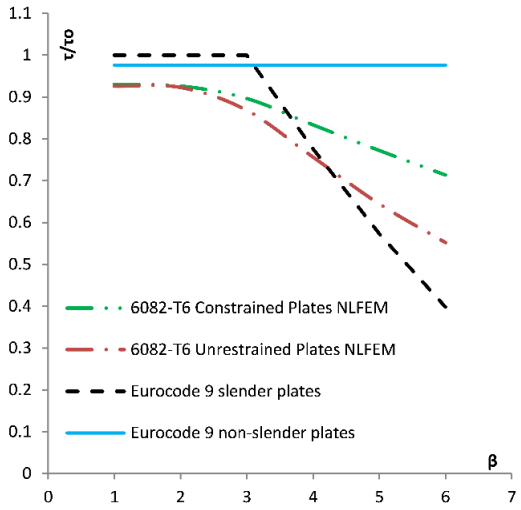

Fig. 32. Comparison of F.E. results of the current study with other theoretical values of the critical shear stress of aluminium alloy 6082-T6 plates under pure shear.

4.2.4.Interaction diagrams of axial compressive/tensile and shear loads for steel, aluminium alloy 5083-H116 and 6082-T6 plates.

Since the complex set of boundary conditions is valid in both cases i.e. under axial compression/tension and under pure shear according to the above comparisons, the same set of boundary conditions was applied to plates under combined loads of axial compression/tension and shear. In cases where either the direct or shear stress components have failed to reach a peak value or have a very flat plateau at collapse, limitations are set for the interaction relationship. In this case, values of either direct or shear stress at strain values ε/εo=2 and γ/γo=2 are used to define the failure stresses for the interaction diagram. These limitations are taken for all the interaction diagrams of steel, aluminium alloy 5083-H116 and 6082-T6 for both cases, unrestrained and constrained edges.

The interaction diagrams of steel plates with unrestrained and constrained edges are depicted in Fig. 33 and Fig. 34, respectively. Fig. 33 shows that very stocky unrestrained steel plates (β=1) follows the Mises yield criterion, according to which $(\sigma/\sigma_o)^2 + (\tau/\tau_o)^2 = 1$ and slender unrestrained plates present high

insensitivity of compressive strength to shear for proportions up to $0.5\tau_o$. In the case of constrained steel plates (Fig. 34), very stocky (β=1) and less stocky plates (β=2, 3) behave in a similar manner to the Mises criterion. The insensitivity of the compressive strength to applied shear remains, but for lower proportions of shear and for very slender plates (β=4, 5, 6). The ultimate and critical shear strength of constrained plates with slenderness ratio (β) higher than 2 under pure axial compression/tension and pure shear is increased in comparison with these of unrestrained plates, as already it has been mentioned in previous sections.

The interaction diagrams of aluminium alloy 5083-H116 plates with unrestrained and constrained edges are depicted in Fig. 35 and Fig.36 respectively. Similar pattern occurs between steel (Fig. 33) and aluminium alloy 5083-H116 (Fig. 35) with unrestrained edges where stocky plates (β=1) follows the Mises yield criterion and very slender plates (β>2) develop high insensitivity to shear. Buckling remains the dominate reason of failure for low proportions of shear to axial compressive load and shear starts to affect plate's strength when it reaches approximately the 50% of shear yield stress. The behaviour of plates with slenderness ratio β=2 is similar to the behaviour of stocky plates but without verifying the Mises yield criterion. The interaction diagram of the constrained aluminium alloy 5083-H116 plates in Fig. 36 does not present particular differences from this of steel constrained plates (Fig. 34). Very stocky plates (β=1) comply with Mises criterion and less stocky plates (β=2, 3) behave in a similar manner. The influence of shear load to the axial compressive strength is greater in the case of slender plates (β=4, 5, 6) and shear buckling occurs for low proportions of shear to direct stress. However, the behaviour of aluminium constrained plates under combined tensile and shear loadings seems to differ from this of steel plates, especially for very slender plates (β=6).

The interaction diagrams of aluminium alloy 6082-T6 plates with unrestrained and constrained edges are depicted in Fig. 37 and Fig. 38, respectively. There no particular differences between the interaction diagrams of aluminium alloys 5083-H116 and 6082-T6. Only, in the case of very slender (β=5, 6) unrestrained aluminium alloy 6082-T6 plates, shear insensitivity occurs for lower proportions of shear than in the same case for aluminium alloy 5083-H116.

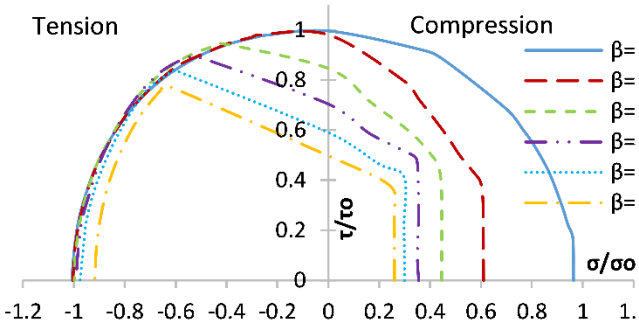

Fig. 33. Interaction diagram of axial compressive/tensile and shear loads for unrestrained steel plates.

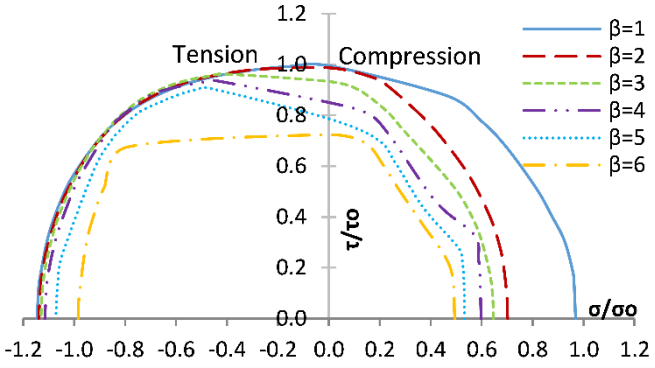

Fig. 34. Interaction diagram of axial compressive/tensile and shear loads for constrained steel plates.

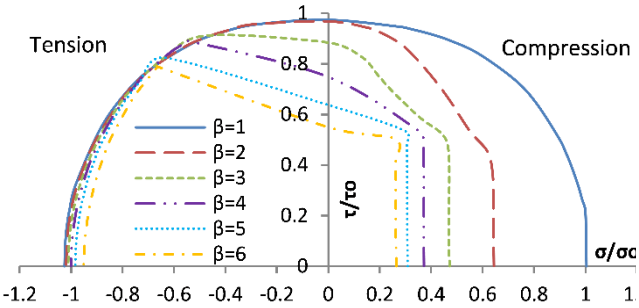

Fig. 35. Interaction diagram of axial compressive/tensile and shear loads for unrestrained aluminium alloy 5083-H116 plates.

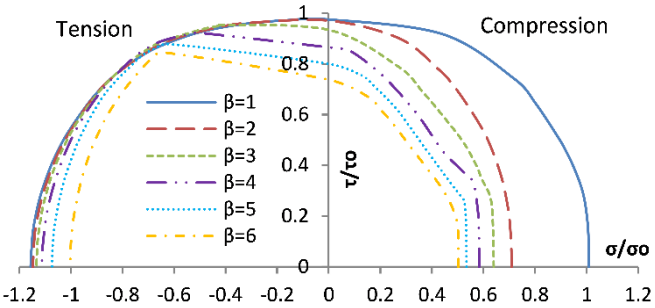

Fig. 36. Interaction diagram of axial compressive/tensile and shear loads for constrained aluminium alloy 5083-H116 plates.

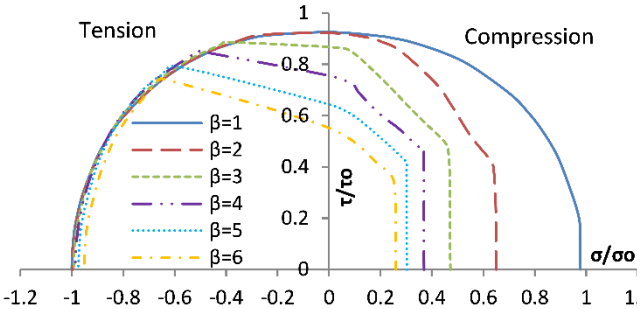

Fig. 37. Interaction diagram of axial compressive/tensile and shear loads for unrestrained 6082-T6 plates.

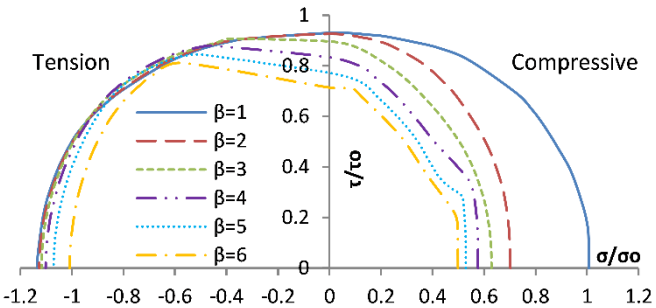

Fig. 38. Interaction diagram of axial compressive/tensile and shear loads for constrained 6082-T6 plates.

5. Conclusions

The progressive collapse assessment of steel and aluminium alloy 5083-H116 and 6082-T6 plates has been investigated under pure shear for plates with aspect ratio (a/b) 1 to 4 and under axial compression/tension, shear and combined compression/tension and shear for square plates.

In the first part, the results of steel and aluminium plates with constrained edges, aspect ratio (a/b) 1 to 4 and slenderness ratio (β) 1 to 5 subjected to pure shear show that the progressive collapse behaviour of plates under pure shear is not affected by the aspect ratio (a/b) of the plates.

In the second part, square plates with slenderness ratio (β) 1 to 6 are subjected to axial compressive/tensile, shear and combined compressive/tensile and shear loads, applying the same boundary conditions. A complex set of boundary conditions for the NLFEM is introduced which allows compressive/tensile and shear loads to be applied simultaneously to ship plating. The effect of constraining the unloaded edges keeping them straight is also investigated. The comparison of the NLFEM results for unrestrained and constrained steel and aluminium plates under axial compression and under shear with theoretical formulas and other studies shows not only the differences between each study/formula, but also the effect of the constrained edges on the ultimate strength of the plates.

The interaction diagrams of axial compressive/tensile and shear load provide the ultimate strength which a plate may sustain under a certain amount of critical shear stress. The results show that the constraints of unloaded edges enhance the ultimate strength of slender plates but not also the strength of stocky plates. Slender constrained plates are more susceptible to shear than unrestrained plates which show high shear insensitivity and buckle due to axial compressive loadings. In addition, steel, aluminium alloy 5083-H116 and 6082-T6 plates of the same slenderness ratio and with the same constraints applied to the unloaded edges follow similar pattern in their interaction diagrams without the material causing particular differences.

Finally, the outcome of this study provides useful information for the progressive collapse of ship plating under axial compression/tension, shear and combined these loads which is essential for further investigation of torsional loads to ship hull girders.

Acknowledgements

This study was performed under an Office of Naval Research grant. The authors would like to thank ONR for their continuing support of this work.

References

[1] P. T. Pedersen, "Beam Theories for torsional-bending response of ship hulls," *J. Ship Res.*, vol. 35, no. 3, pp. 254–265, 1991.
[2] S. Benson, "Progressive Collapse Assessment of Lightweight Ship Structures," Newcastle University, 2011.
[3] D. Faulkner, "A review of effective plating for use in the analysis of stiffened plating in bending and compression," *J. Ship Res.*, vol. 19, pp. 1–17, 1975.
[4] P. A. Frieze, P. J. Dowling, and R. E. Hobbs, "Ultimate Load Behaviour of Plates in Compression," in *Steel Plated Structures*, London: Crosby Lockwood Staples, 1977, pp. 24–50.
[5] R. S. Dow and C. S. Smith, "Effects of Localized Imperfections on Compressive Strength of Long Rectangular Plates," *J. Constr. Steel Res.*, vol. 4, pp. 51–76, 1984.
[6] C. S. Smith, P. C. Davidson, J. C. Chapman, and P. J. Dowling, "Strength and stiffness of ships plating under in-plane compression and tension," *R. Inst. Nav. Archit.*, 1987.
[7] D. W. Chalmers, *Design of Ships' Structures*. London: HMSO, 1993.
[8] G. H. Little, "Collapse behaviour of aluminium plates," *Int. J. Mech. Sci.*, vol. 24, no. 1, pp. 37–45, Jan. 1982.
[9] D. S. Mofflin and J. B. Dwight, "BUCKLING OF ALUMINIUM PLATES IN COMPRESSION," 1984, pp. 397–427.
[10] Eurocode 9 EN 1997-1-1, "Design of Aluminium Structures, part 1.1 General structural rules," London: British Standard Institution, 2007.
[11] O. S. Hopperstad, M. Langseth, and T. Tryland, "Ultimate strength of aluminium alloy outstands in compression: experiments and simplified analysis," *Thin-Walled Struct.*, vol. 34, no. 4, pp. 279–294, 1999.
[12] O. H. H. Kristensen, "Ultimate Capacity of Aluminium Plates under Multiple Loads, considering HAZ Properties," NTNU, Trondheim, 2001.
[13] J. Paik and A. Duran, "Ultimate Strength of Aluminium Plates and Stiffened Panels for Marine Applications," *Mar. Technol.*, vol. Vol.41, no. No. 3, pp. 108–121, Jul. 2004.
[14] S. Zhang, P. Kumar, and S. E. Rutherford, "Ultimate shear strength of plates and stiffened panels," *Ships Offshore Struct.*, vol. 3, no. 2, pp. 105–112, May 2008.
[15] S. Nara, Y. Deguchi, and Y. Fukumoto, "ULTIMATE STRENGTH OF STEEL PLATE PANELS WITH INITIAL IMPERFECTIONS UNDER UNIFORM SHEARING STRESS.," *Doboku Gakkai Rombun-Hokokushu Proceedings Jpn. Soc. Civ. Eng.*, vol. 9, no. 4, pp. 265–271, 1988.
[16] J. K. Paik, A. K. Thayamballi, and B. J. Kim, "Advanced ultimate strength formulations for ship plating under combined biaxial compression/tension, edge shear, and lateral pressure loads," *Mar. Technol.*, vol. 38, no. 1, pp. 9–25, 2001.

[17] Eurocode 3 ENV 1993-1-1, “Design of steel structures, part 1.1 General rules and rules for buildings,” London: British Standard Institution, 2005.
[18] J. E. Harding, R. E. Hobbs, and B. G. Neal, “Ultimate Load Behaviour of Plates under Combined Direct and Shear In-plane Loading,” in *Steel Plated Structures*, London: Crosby Lockwood Staples, 1977, pp. 369–404.
[19] Adrian F. Dier, “Comparisons of Steel and Aluminium Plate Strengths,” in *Proceeding of the International Conference on Steel and Aluminium Structures*, Cardiff, UK, 1987.
[20] M. M. Alinia, H. R. Habashi, and A. Khorram, “Nonlinearity in the postbuckling behaviour of thin steel shear panels,” *Thin-Walled Struct.*, vol. 47, no. 4, pp. 412–420, 2009.
[21] J. Paik and A. Thayamballi, *Ultimate limit state design of steel-plated structures*. Chichester, UK: John Wiley & Sons Ltd, 2003.